Orthonormal Wavelet Bases for Quantum Molecular Dynamics

C. J. Tymczak and Xiao-Qian Wang

Department of Physics & Center for Theoretical Studies of Physical Systems, Clark Atlanta University, Atlanta, Georgia 30314

(Received 7 October 1996)

We report on the use of compactly supported, orthonormal wavelet bases for quantum molecular-dynamics (Car-Parrinello) algorithms. A wavelet selection scheme is developed and tested for prototypical problems, such as the three-dimensional harmonic oscillator, the hydrogen atom, and the local density approximation to atomic and molecular systems. Our method shows systematic convergence with increased grid size, along with improvement on compression rates, thereby yielding an optimal grid for self-consistent electronic structure calculations. [S0031-9007(97)03146-3]

PACS numbers: 31.15.–p, 02.70.Rw

Recent advances in *ab initio* calculational methods have experienced a considerable amount of success in predicting ground-state structural and cohesive properties of condensed-matter systems [1]. The pioneering work of Car and Parrinello [2], based on dynamical simulated annealing, promoted a new class of approaches [3] applicable to density-functional theory within the local-density approximation (LDA) [4]. Density-functional molecular dynamics (Car-Parrinello) [2] and other iterative methods [5] based on plane-wave basis have made such calculations possible for systems consisting of several hundred atoms [6]. While these methods have been very successful, several difficulties arise when they are extended to systems with large length scales or those containing transition-metal atoms. Several recently proposed techniques such as optimized pseudopotentials, adaptive coordinates, and preconditioning combined with conjugate-gradient techniques have had considerable success [5–7]. Yet, these approaches are still constrained by the plane-wave-basis set which relies on the fast Fourier transform (FFT) to effectively transform between real and reciprocal spaces.

Recently, it has been recognized [8–10] that it may be advantageous to perform electronic structure calculations using a wavelet basis that has dual localization characteristics in real and reciprocal spaces. One of the important features of the wavelet basis is its ability to reduce the number of components needed for solving the Kohn-Sham equation [11], reminiscent of compression in applying wavelets to image processing [12]. Furthermore, multiresolution analysis provides automatic preconditioning [6] on all length scales, which increases the rate of convergence of the electronic wave functions.

Arias and coworkers [8] employed a tight frame generated by the Mexican hat wavelet and applied it to electronic structure calculations. Their work represents an extension of multiresolution analysis to nonorthogonal bases. The generalized multiresolution analysis, utilizing a Gaussian scaling function and the Mexican hat wavelet, turns out to be a very good approximation in representing the electronic wave functions. However, the corresponding inverse transform necessary for the self-consistent calculations is complicated [8,13].

Wei and Chou [9] have devised a method for using compactly supported orthogonal wavelets, developed by Daubechies ($\mathcal{D}_6$) [12], for self-consistent electronic structure calculations. This approach takes advantage of the existence of a fast, discrete wavelet transform (DWT) [14] associated with the Daubechies wavelets. They have demonstrated that the resulting Hamiltonian matrix in wavelet space can be reduced by a factor of hundreds, making it feasible for obtaining the eigenvalues and eigenfunctions through standard diagonalization. While the preliminary application of this method in atomic and molecular systems is promising, there remain several important issues relevant to practical applications. These include the selection of the wavelet components, the effective construction of the matrix elements of the local pseudopotential, and the convergence of the electronic wave functions.

The selection of the wavelet components is a key unsolved issue in applying wavelet bases to electronic structure calculations. In principle, the selection should be based on the eigenfunctions of the Hamiltonian matrix, i.e., the outcome of the diagonalization process. However, the eigenfunctions are not known *a priori*. Approximate methods, e.g., using the wavelet transform of the local potential as a guide [9], may not guarantee the selected wavelet components being optimal. This may further lead to problems in convergence of the electronic wave functions. It is also worth pointing out that the representation of the local pseudopotential in the wavelet space is of a complicated form and amounts to an $O(N_g^2)$ process for a system of N_g grid points. This severely hampers the practical applicability of their method [9].

In this Letter we report on the use of the Daubechies wavelet bases ($\mathcal{D}_6$-$\mathcal{D}_{14}$) in the Car-Parrinello (CP) algorithm [2]. Our approach preserves the advanced features of the CP method, and the transform between the real and wavelet spaces can be efficiently carried out using the DWT. The DWT associated with the wavelets of compact support has many similarities to FFT. Both

 0031-9007/97/78(19)/3654(4)$10.00

are unitary and scale as $N_g \log N_g$. The primary advantage of DWT over FFT is the capability of representing the wave functions with a minimal number of components that scales as $N_{\rm W} \sim \log N_g$. Using the CP method, the calculations associated with the local pseudopotential—a predominant part in the self-consistent calculations—are then $O(N_g)$ for each energy level. In addition, the construction of the separable nonlocal pseudopotential matrix elements of the Kleinman-Bylander form [15] scales as $O(N_{\rm W}^2)$, while the matrix elements of the kinetic energy can be obtained through transformation of a band-diagonal matrix into wavelet space [9,16].

Wavelets are very useful in representing data or functions [13]. An orthonormal wavelet is generated by an analyzing wavelet and an auxiliary function called the scaling function. The basis is constructed from the analyzing wavelet and scaling function by the operations of translations and dyadic dilations. Unlike the sines and cosines that comprise the bases in Fourier analysis, which are localized in Fourier space but delocalized in real space, both mother wavelet and scaling function are dual localized in real and reciprocal spaces [12].

The CP method [2] involves a fictitious molecular dynamics solution of electronic wave functions on the Born-Oppenheimer surface,

$$\mu \ddot{\Psi}_i(t) = -H\Psi_i(t) + \sum_l \Lambda_{il}\Psi_l(t), \qquad (1)$$

where μ is a fictitious mass and Λ_{il} are the Lagrange constraints. The Gram-Schmidt orthogonalization scheme is employed to keep the wave functions of the occupied states orthogonal. It is known that the calculation of nonlocal pseudopotentials and the orthogonalization process (using either Gram-Schmidt or iterative solutions) are bottlenecks in plane-wave based calculations. The use of orthonormal wavelet bases is capable of reducing the cost for these calculations. In fact, for both types of calculations, the compression associated with the wavelet bases is most beneficial in that an $O(N_g^2)$ process can be reduced to $O(N_W^2)$.

With the use of orthonormal wavelet bases for the expansion of wave functions, the corresponding matrix representation of the Hamiltonian consists of kinetic and potential energy parts. Choosing the three-dimensional wavelet as a combination of three one-dimensional wavelets, the kinetic matrix factors into products of three submatrices of x, y, and z components, which can be readily calculated and tabulated beforehand [16]. The construction of the potential energy matrix in wavelet space entails (i) calculating $V_{\rm eff}\Psi$ for each occupied energy level in real space, and (ii) transforming the product back into wavelet space. For electronic structure calculations, an inverse wavelet transform of the resulting wave functions are needed to construct $V_{\rm eff}$ of the Kohn-Sham Hamiltonian [4].

We have developed a "bootstrap" algorithm for selecting the significant wavelet components. The wavelet components of a continuous function $u(x)$, at scale j, are of the form:

$$d_{jk} = \int dx\, u(x)\; 2^{-j/2}\psi(2^{-j}x - k), \qquad (2)$$

where ψ is the analyzing wavelet. For an orthonormal wavelet with M vanishing moments ($\mathcal{D}_M$), the wavelet components at scale $(j-1)$ are related to those at (coarser) scale j by

$$d_{j-1,k} \approx 2^{-(M+\frac{1}{2})} d_{j,k}, \qquad (3)$$

provided that one can neglect the Taylor series expansion of $u(x)$ to orders greater than M. As an example, we show in Fig. 1 the wavelet coefficients for a Gaussian function using the $\mathcal{D}_8$ wavelet. The scaling behavior of the coefficients is readily observable, which constitutes the basis of compression in the context of image processing.

Taking advantage of the scaling behavior described above, we start by solving for the (unknown) wave function in wavelet space using the coefficients from the coarsest scale (J) to scale j. Next, we select the important wavelet coefficients from this subset of coefficients by removing those below the (predetermined) threshold tolerance. Then, at scale $j-1$, only those coefficients that are connected with the surviving components at scale j need to be considered further for sorting. This procedure is repeated until the finest scale is reached.

A few remarks are in order. In contrast to the simple sorting scheme used by other applications [9], the "bootstrap" algorithm is efficient in that any negligible component at a coarse scale results in the elimination of the associated components at finer scales. It is worth noting that this algorithm provides preconditioning [6] on the finer

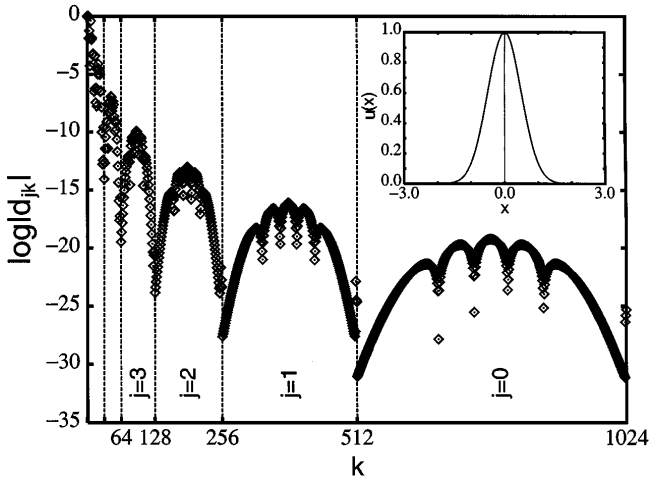

FIG. 1. Wavelet components of a Gaussian function (inset plot) using $\mathcal{D}_8$. The dashed lines correspond to the boundaries between each scale (labeled by j).

TABLE I. The kinetic, potential, and total energies ($E_{\rm kin}$, $E_{\rm pot}$, and $E_{\rm tot}$) of the harmonic oscillator in units of ω_0, calculated with different wavelets ($\mathcal{D}_6$, $\mathcal{D}_8$, and $\mathcal{D}_{14}$) for different grid size (N_g) and the requested wavelet components ($N_{\rm W}$).

N_g	Wavelet	$N_{\rm W}$	$E_{\rm kin}$	$E_{\rm pot}$	$E_{\rm tot}$
16^3	$\mathcal{D}_6$	3101	0.4955596	0.5180191	1.0135787
	$\mathcal{D}_8$	3009	0.4986462	0.5031520	1.0017982
	$\mathcal{D}_{14}$	2680	0.4999382	0.5000889	1.0000276
32^3	$\mathcal{D}_6$	4724	0.4994644	0.5016613	1.0011258
	$\mathcal{D}_8$	3764	0.4998524	0.5002569	1.0001093
	$\mathcal{D}_{14}$	3341	0.4999917	0.5000093	1.0000009
64^3	$\mathcal{D}_6$	3996	0.4997000	0.5006009	1.0003004
	$\mathcal{D}_8$	3644	0.4998777	0.5002089	1.0000867
	$\mathcal{D}_{14}$	3584	0.4999938	0.5000062	1.0000000

scales. Most importantly, the dynamic simulated annealing procedure for solving the eigenfunctions allows, at the same time, the selection of important wavelet components without the necessity of resorting to approximations.

For purposes of demonstrating our approach, we apply the method to the three-dimensional harmonic oscillator. Table I shows our results for the system at various grid sizes, using Daubechies wavelets with varying supports. As seen from Table I, a systematic convergence to the exact result is achieved with increasing grid size and/or with the use of smoother wavelets of wider supports, along with the notable improvement of the compression rate (as measured by N_W/N_g). For instance, using the $\mathcal{D}_{14}$ wavelet at a grid size of 64^3, the eigenvalue convergence is better than 10^{-10} with a compression rate of about 1%.

An important ramification of these results is the stability of our algorithm. The systematic convergence indicates that the bootstrap algorithm is a controlled selection procedure. We have verified the systematic convergence of our algorithm for the harmonic oscillator, the hydrogen atom (see Table II), and the self-consistent electronic structure calculations utilizing pseudopotentials. For illustration, we list in Tables III and IV results for LDA calculations with the pseudopotentials for the helium atom and hydrogen dimer. These results demonstrate that for relatively smooth potentials, our algorithms converges systematically with increasing grid size, with improving compression rates (the typical compression rate for a 128^3 system is about 0.2%).

TABLE III. The calculated total energy (in Rydberg) of atomic helium with different grid size (N_g) and the corresponding compression rate ($N_{\rm W}/N_g$).

System	N_g	$N_{\rm W}/N_g$	$E_{\rm LDA}$ (present work)	$E_{\rm LDA}$
Helium	32^3	17.6%	−1.978	−2.814
	64^3	2.3%	−2.400	
	128^3	0.3%	−2.635	
Pseudo	32^3	21.4%	−2.536	−2.831
	64^3	2.4%	−2.785	
	128^3	0.3%	−2.792	

It is worthwhile to compare CP methods using traditional plane-wave and wavelet bases in order to evaluate the efficiency of our approach. For a single iteration, this amounts to comparing the relative speed between FFT and DWT. Our best optimized DWT is three times slower than the FFT. Although there is room for further optimizing the DWT, this is not the main thrust of the present Letter. As a result, for relatively small systems (e.g., harmonic oscillator at size 16^3), the plane-wave code outperforms our algorithm. This is, however, no longer the case for larger systems (e.g., harmonic oscillator at 64^3) because the wavelet algorithm yields much faster convergence rate, which can be attributed to the drastic reduction in the number of local minima.

For a better understanding of how our method works, we consider all-electron calculations with the Coulomb potential. We employ a simple approximation to the singular Coulomb potential by replacing it with a nonsingular one of the form $Zerf(r/\sigma)/r$, where σ is chosen to cover only the nearest neighbor points. This potential guarantees the ground state energy to be an upper bound, and a better approximation of the original Coulomb potential with increasing grid size. It is important to point out that this choice of the potential is not for obtaining accurate energies for systems like the hydrogen atom, which is well known and can be properly handled by other methods [10]. Rather, we wish to use this exercise to explore the applicability of our approach to singular potentials. Figure 2 shows the radial part of the calculated ground

TABLE II. The kinetic, potential, and total energies ($E_{\rm kin}$, $E_{\rm pot}$, and $E_{\rm tot}$) of the hydrogen atom in atomic units and the compression rate ($N_{\rm W}/N_g$), calculated using $\mathcal{D}_8$ for different grid size (N_g).

N_g	$N_{\rm W}/N_g$	$E_{\rm kin}$	$E_{\rm pot}$	$E_{\rm tot}$
16^3	57.9%	0.40484	−1.23225	−0.82740
32^3	13.4%	0.58328	−1.48928	−0.90599
64^3	2.1%	0.71455	−1.66780	−0.95325
128^3	0.3%	0.78551	−1.76712	−0.98161

TABLE IV. Calculated bond length (d) and vibrational frequencies (ν) of the diatomic H_2 using the Murnaghan equation of state. Experimental results from Ref. [14] are included for comparison.

	Grid	d (a.u.)	ν ($\rm cm^{-1}$)
Modified Coulomb	64^3	1.62	3820
Modified Coulomb	128^3	1.52	4390
Pseudopotential	64^4	1.57	4180
Experiment		1.40	4400

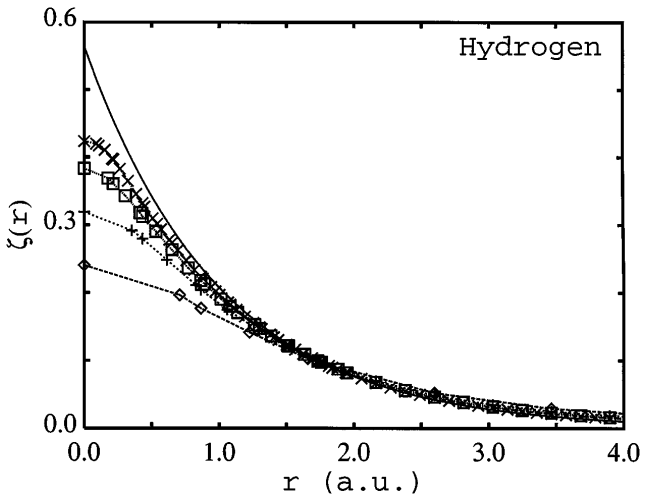

FIG. 2. The radial part of the hydrogen atom's ground state eigenfunction calculated on a grid of 16^3 (◇), 32^3 (+), 64^3 (□), and 128^3 (×) as compared to the analytical solution (solid line).

state wave function for the hydrogen atom with respect to different grid sizes, as compared to the exact solution. The major deviation from the analytical solution occurs, as expected, around the ionic core region. Our calculation clearly shows that, with an increase of the grid size, the algorithm picks up more wavelet components around the ionic core region, thereby improving the results. Similar behavior is also observed for the helium atom (see Table III).

Table IV shows the results for the hydrogen dimer at different grid sizes with use of the simplified potential and the hydrogen pseudopotential. Figure 3 shows the representative curves and data points used to calculate the bonding length and vibrational frequency. Our calculation using the simplified potential on a 128^3 grid yielded reasonably better results, indicating that the wavelet basis is capable of handling singular potentials, even with simple approximations.

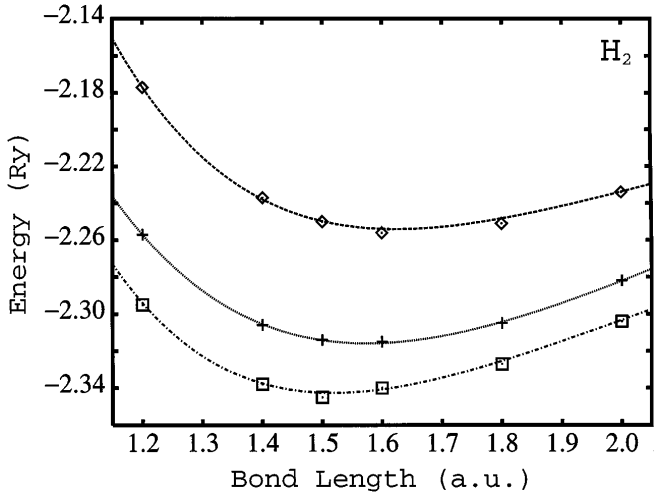

FIG. 3. Calculated total energy of H_2 as a function of bond length using pseudopotential (+), and all-electron calculation with different grid size [(◇) for 64^3 and (□) for 128^3, respectively]. The curves are fits of the Murnaghan equation of states of the calculated points.

In summary, we have presented a method that permits us to perform quantum molecular dynamics simulations based on orthonormal wavelet bases. We have developed an efficient scheme for the selection of important wavelet components. The advantage of using a dynamical simulated annealing lies in the fact that it is not only making the selection of the components a controlled procedure, but also offering a natural way for reducing the cost in comparison with plane-wave based calculations.

Fruitful discussions with M. Y. Chou, C. R. Handy, R. Murenzi, and S. Wei are gratefully acknowledged. This work was supported in part by the National Science Foundation under Grant No. HRD9450386, Air Force Office of Scientific Research under Grant No. F49620-96-1-0211, and Army Research Office under Grant No. DAAH04-95-1-0651.

[1] See, for instance, R. G. Parr and W. Yang, *Density Functional Theory of Atoms and Molecules* (Oxford University Press, Oxford, 1989).
[2] R. Car and M. Parrinello, Phys. Rev. Lett. **55**, 2471 (1985).
[3] M. C. Payne, M. P. Teter, D. C. Allan, T. A. Arias, and J. D. Joannopoulos, Rev. Mod. Phys. **64**, 1045 (1992), and references therein.
[4] W. E. Pickett, Comput. Phys. Rep. **9**, 115 (1989); O. H. Nielsen and R. M. Martin, Phys. Rev. Lett. **50**, 697 (1983).
[5] D. Vanderbilt, Phys. Rev. B **41**, 7892 (1990).
[6] J. R. Chelikowsky, N. Troullier, and Y. Saad, Phys. Rev. Lett. **72**, 1240 (1994).
[7] W. Kohn and L. J. Sham, Phys. Rev. **140A**, 1133 (1965).
[8] T. A. Arias, K. J. Cho, P. K. Lam, and M. P. Teter, in *Toward Teraflop Computing and New Grand Challenge Applications*, edited by P. K. Kalia and P. Vashishta (Nova Scientific Publications, Commack, 1995), p. 23; K. Cho, T. A. Arias, J. D. Joannopoulos, and P. K. Lam, Phys. Rev. Lett. **71**, 1808 (1993).
[9] S. Wei and M. Y. Chou, Phys. Rev. Lett. **76**, 2650 (1996).
[10] K. Yamaguchi and T. Mukoyama, J. Phys. B **29**, 4059 (1996).
[11] G. Beylkin, SIAM J. Numer. Anal. **6**, 1716 (1992).
[12] I. Daubechies, *Ten Lectures on Wavelets* (Society for Industrial and Applied Mathematics, Philadelphia, 1992).
[13] J-P. Antoine and R. Murenzi, in *Subband and Wavelet Transforms*, edited by A. N. Akansu and Mark J. T. Smith (Kluwer Academic Publishers, 1996).
[14] I. Daubechies, Commun. Pure Appl. Math. **41**, 909 (1988).
[15] L. Kleinman and D. M. Bylander, Phys. Rev. Lett. **48**, 1425 (1982).
[16] G. Beylkin, SIAM J. Numer. Anal. **6**, 1716 (1992); G. Beylkin, R. Coifman, and V. Rokhlin, Commun. Pure Appl. Math. **44**, 141 (1991).